Effect of window reflections on photonic Doppler velocimetry measurements

T. Ao[a)] and D. H. Dolan
Sandia National Laboratories, Albuquerque, New Mexico 87185, USA

(Received 10 November 2010; accepted 6 January 2011; published online 24 February 2011)

Photonic Doppler velocimetry (PDV) has rapidly become a standard diagnostic for measuring velocities in dynamic compression research. While free surface velocity measurements are fairly straightforward, complications occur when PDV is used to measure a dynamically loaded sample through a window. Fresnel reflections can severely affect the velocity and time resolution of PDV measurements, especially for low-velocity transients. Shock experiments of quartz compressed between two sapphire plates demonstrate how optical window reflections cause ringing in the extracted PDV velocity profile. Velocity ringing is significantly reduced by using either a wedge window or an antireflective coating. © *2011 American Institute of Physics*. [doi:10.1063/1.3551954]

I. INTRODUCTION

Optical velocimetry is a powerful diagnostic for probing the response of materials under shock[1–3] and isentropic[4–6] compression. Photonic Doppler velocimetry (PDV), also known as heterodyne velocimetry,[7,8] is a compact displacement interferometer system that has steadily gained use in dynamic loading experiments. It has many of the advantages of velocity interferometer system for any reflector (VISAR) (Refs. 9 and 10) and Fabry–Pérot interferometry,[11,12] while avoiding some their disadvantages. PDV is essentially fiber-based Michelson interferometry, utilizing recent advances in near-infrared ($\lambda_0 = 1550$ nm) detector technology and fast digitizers to record beat frequencies in the gigahertz (GHz) range. While light return fluctuations are observed in the data, PDV is robust against large intensity variations. The use of Fourier transform techniques[13–15] in the analysis of PDV data enable resolving multiple discrete velocities and even velocity dispersion. Additional advantages of PDV include simple assembly and operation, readily available components, and lack of an intrinsic delay time.

Free surface velocities of shocked samples have been successfully obtained using PDV.[16–20] PDV measurements can also be performed through an optical window to maintain a high pressure state in the sample, though optical reflections within the window lead to multiple apparent velocities.[21] In many cases, PDV analysis over long time scales provides adequate separation of the overtones from the primary velocity of interest. However, considerable overlap occurs for short-time scale analysis, causing severe velocity resolution loss.

This work investigates the effects of window reflections on PDV performance. Emphasis is placed on modest velocities (<1 km/s), where overtone overlap issues are particularly acute. Section II provides a theoretical discussion of window reflections in PDV measurements. Section III describes impact experiments that test the theoretical predictions; results and analysis of these experiments are presented in Sec. IV. Section V discusses the resolution limits that window reflections place upon PDV in comparison with the performance of VISAR. A summary of the work is given in Sec. VI.

II. CONCEPTUAL BACKGROUND

PDV signals are typically analyzed in the velocity-mode procedure described by Jensen *et al.*[21] The measured signal $s(t)$ is converted to a time-frequency representation $\tilde{S}(f,\bar{t})$ using a short-time Fourier transform (STFT) (Refs. 14 and 22)

$$\tilde{S}(f,\bar{t}) \equiv \int_{-\infty}^{\infty} w(t-\bar{t})\, s(t)\, e^{-2\pi i f t}\, dt. \tag{1}$$

At each time point $\bar{t}$, a digital window[15] function $w(t)$ limits the Fourier transform to a local duration τ ($w = 0$ for $|t-\bar{t}| \geq \tau/2$). The value of τ is related to the characteristic peak width Δf of $|\tilde{S}|^2$ by the uncertainty principle

$$(\Delta f)(\tau) > 1/4\pi. \tag{2}$$

For example, STFT analysis using $\tau = 5$ ns yields a minimum frequency width of 0.0159 GHz, which corresponds to a velocity width of 12.3 m/s at $\lambda_0 = 1550$ nm. Peak position can be defined more narrowly than the width for single-frequency signals,[23] but the uncertainty principle remains important in multi-frequency signals because it defines the overlap between frequency components.

Consider a PDV measurement through an optical window as shown in Fig. 1. The left side of the window is coated with a reflector, and light enters the window from the right. Some light (path "0") is reflected at the window free surface (which remains at rest), while most light travels to the reflector. Light returning to the free surface may be transmitted (path "1") or reflected for another window transit (path "2"). Additional window transits also contribute to the measurement, but their influence is progressively weaker with each transit (due to Fresnel loss and probe efficiency). For simplicity, the window is assumed to be perfectly transparent at 1550 nm for any compression state.

The optical phase of the kth reflection is related to the input phase $\phi_A = 2\pi f_A t + \delta_A$ as follows:

$$\phi_k(t) = \begin{cases} \phi_A(t-2T_v) & k=0 \\ \phi_A(t-2T_v-2kT_w(t)) - \delta_k & k>0. \end{cases} \tag{3}$$

[a)]Electronic mail: tao@sandia.gov.

 © 2011 American Institute of Physics

Downloaded 30 Mar 2011 to 198.102.153.2. Redistribution subject to AIP license or copyright; see http://rsi.aip.org/about/rights_and_permissions

Transit times T_v and $T_w(t)$ describe the passage of light in vacuum and window (respectively), the former remaining constant while the free surface is at rest. Phase shifts δ_k describe constant changes that accumulate for each reflection at the sample–window interface and window–vacuum interface. Each reflected phase is mixed with a reference phase $\phi_R(t) = 2\pi f_R t + \delta_R$ in the PDV, so the phase differences are

$$\Phi_k(t) = 2\pi f_C t - 4\pi f_A T_w(t) + \Delta_k. \tag{4}$$

The conversion frequency f_C is the difference between the target and reference sources ($f_C = f_A - f_R$); Δ_k is a collection of constants (phase shifts, etc.) for a specific reflection. For a reflector moving at a constant apparent velocity ($v^* \ll c_0$), the phase difference may be approximated as

$$\Phi_k(t) = 2\pi(\underbrace{f_C + kf_D}_{f_k})t + \Delta_k, \tag{5}$$

where the Doppler shift frequency is given as $f_D = 2v^*/\lambda_0$. The window is assumed to be linear[24] so that the apparent velocity scales directly with the actual velocity.

If the reference intensity is much stronger than any of the reflected intensities, the measured PDV signal (AC coupled) containing $N + 1$ frequency components is given as

$$s(t) = \sum_{k=0}^{N} A_k \cos(2\pi f_k t + \Delta_k). \tag{6}$$

The signal contribution of each reflection is weighted by A_k (field amplitude ratio), discarding common scaling factors (such detector responsivity). All reflections may be scaled with respect to the primary reflection ($A_1 = 1$), with A_k generally less than unity. Note that the field amplitude ratio is the square root of the intensity ratio: if the power collected from a harmonic is 1% of the primary, the value of A_k is 10%.

Neglecting overall phase, the STFT of Eq. (6) is

$$\tilde{S}(f,\bar{t}) = \sum_{k=0}^{N} \frac{A_k}{2}\{e^{+i\gamma_k(\bar{t})}S_{+f_k}(f) + e^{-i\gamma_k(\bar{t})}S_{-f_k}(f)\},$$
$$S_{\pm f_k}(f) \equiv \int_{-\infty}^{\infty} w(q)e^{\pm 2\pi i(f\mp f_k)q}\,dq, \tag{7}$$

where $\gamma_k(\bar{t}) \equiv 2\pi f_k \bar{t} + \Delta_k$. The square-magnitude of the STFT (power spectrum) of the PDV signal is

$$\begin{aligned}|\tilde{S}(f,\bar{t})|^2 \propto &\sum_{k=0}^{N} A_k^2\{S_{+f_k}^2(f) + S_{-f_k}^2(f) + 2\cos[2\gamma_k(\bar{t})]S_{+f_k}(f)S_{-f_k}(f)\}\\ &+2\sum_{k=0}^{N}\sum_{j=k+1}^{N} A_kA_j\cos[\gamma_k(\bar{t}) - \gamma_j(\bar{t})]\{S_{+f_k}(f)S_{+f_j}(f) + S_{-f_k}(f)S_{-f_j}(f)\}\\ &+2\sum_{k=0}^{N}\sum_{j=k+1}^{N} A_kA_j\cos[\gamma_k(\bar{t}) + \gamma_j(\bar{t})]\{S_{+f_k}(f)S_{-f_j}(f) + S_{-f_k}(f)S_{+f_j}(f)\}.\end{aligned} \tag{8}$$

Each frequency in the signal contains a positive and a negative frequency component, which leads to three general contributions to the power spectrum:

(1) Positive, negative, and cross-sign products of the frequency peak for each component.
(2) Same-sign cross products of different components.
(3) Opposite-sign cross products of different components.

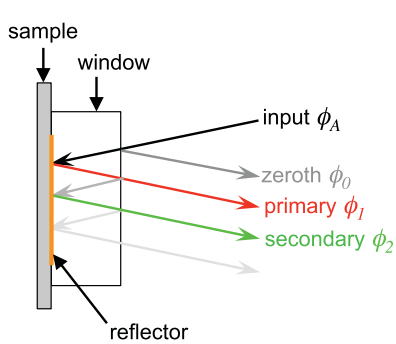

FIG. 1. (Color) Fresnel window reflections of PDV light.

The shape and width of each frequency component depends upon the digital window function: narrow digital windows lead to broad frequency components and *vice versa*.

Consider a PDV measurement containing three Doppler shifts at beat frequencies f_0, f_1, f_2, corresponding to zeroth, primary, and secondary reflections, respectively, ($f_k = f_C + kf_D$, $k = 0, 1, 2$). Figure 2(a) illustrates a pictorial representation of these frequency components obtained with conventional PDV ($f_C = 0$) using a narrow digital window. Equation (8) indicates that the power spectrum of a three frequency PDV signal contains six static contributions (spectral functions centered at $+f_0, -f_0, +f_1, -f_1, +f_2, -f_2$) and nine time-dependent contributions. Table I summarizes the location, time dependence, and relative strength of each contribution. The contribution $A_1^2 S_{+f_1}^2(f)$ centered at $+f_1$ corresponds to the primary reflection, and is assumed to be the strongest reflection and the "main" feature of interest. However, adjacent positive frequency peaks at f_0 and f_2 have a non-negligible influence in this area, both as static and time-dependent perturbations in the overall spectrum. Negative frequency components may

Downloaded 30 Mar 2011 to 198.102.153.2. Redistribution subject to AIP license or copyright; see http://rsi.aip.org/about/rights_and_permissions

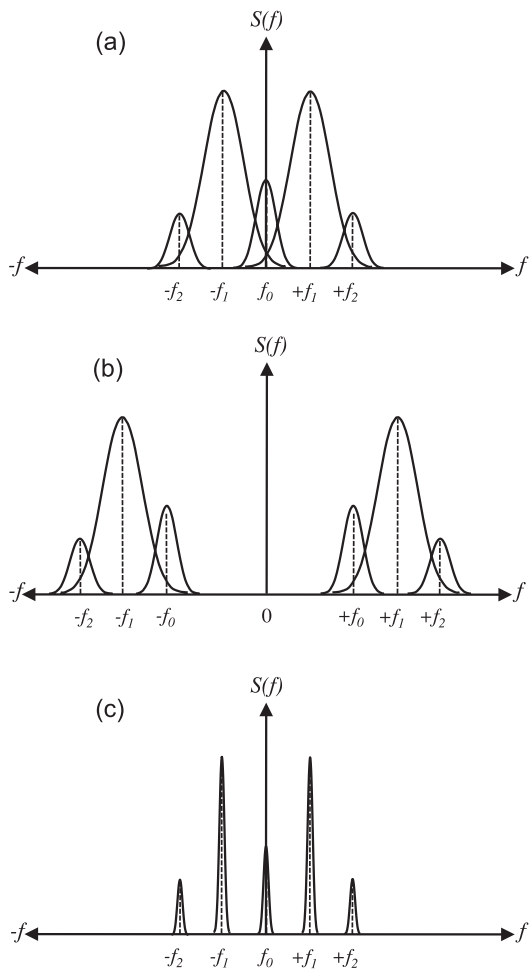

FIG. 2. Spectral functions of (a) conventional PDV with a small analysis time duration τ, (b) frequency-conversion PDV with a small τ, and (c) conventional PDV with a large τ. When the window–vacuum surface is at rest, $f_0 = 0$ for conventional PDV and $f_0 = f_C$ for frequency-conversion PDV.

also play a role in the power spectrum, even at positive frequencies.

The relative impact of each frequency component depends on several factors. The signal magnitude A_k obviously plays a role. The overlap between a particular component and the $+f_1$ peak is also important. Large values of $+f_1$ separate the positive and negative components, reducing the perturbations of the latter at positive frequencies. This separation occurs naturally for large velocity changes and can also be created through the use of frequency-conversion ($f_C \neq 0$) as shown in Fig. 2(b). Spectral overlap may be reduced by increasing the digital window width, creating narrower peaks as shown in Fig. 2(c), at the expense of time resolution. Reducing spectral overlap benefits PDV performance in two ways. Static contributions systematically alter the power spectrum, reducing accuracy by biasing the peak away from $+f_1$. Time dependent contributions vary the power spectrum about its mean value, reducing precision.

III. EXPERIMENTAL METHOD

Figure 3 shows the layout of experiments performed to examine the effect of window reflections on PDV measurements. A single-stage gas gun was used to launch a c-axis sapphire impactor (25.4 mm diameter, 6.3 mm thick) at a target which consisted of a z-axis quartz sample (29.2 mm diameter, 0.5 mm thick) backed by a c-axis sapphire window (25.4 mm diameter, 12.8 mm thick). Since the sample is sandwiched between two higher impedance materials, the sample-window interface experienced a well-defined reverberation history: an initial step, followed by two subsequent steps, over roughly 500 ns.

The interior side of the sapphire window was coated with a 3 mm diameter Al reflector (≈300 nm thick); the

TABLE I. Static and dynamic terms in a PDV signal containing three Doppler shifts (zeroth, primary, and secondary reflections). The relative strength assignment is based on the overall magnitude (e.g., A_0^2), with the assumption that the primary reflection is the strongest. Static terms are strongly peaked at single center frequency, while dynamic terms are products of two spectral functions (peaked at different center frequencies) with an overall oscillation at the ringing frequency. The box indicates the main feature of interest, the primary reflection, the remaining terms interfere with measurements of $+f_1$.

Static terms in Eq. (8)	Relative strength	Center frequency
$A_0^2 S_{+f_0}^2(f)$	Weak	$+f_0$
$A_0^2 S_{-f_0}^2(f)$	Weak	$-f_0$
$A_1^2 S_{+f_1}^2(f)$	Strong	$\boxed{+f_1}$
$A_1^2 S_{-f_1}^2(f)$	Strong	$-f_1$
$A_2^2 S_{+f_2}^2(f)$	Weak	$+f_2$
$A_2^2 S_{-f_2}^2(f)$	Weak	$-f_2$
Dynamic terms in Eq. (8)	**Relative strength**	**Ringing frequency**
$2A_0^2 S_{+f_0}(f) S_{-f_0}(f)$	Weak	$2f_0 = 2f_C$
$2A_1^2 S_{+f_1}(f) S_{-f_1}(f)$	Moderate	$2f_1 = 2f_C + 2f_D$
$2A_2^2 S_{+f_2}(f) S_{-f_2}(f)$	Weak	$2f_2 = 2f_C + 4f_D$
$2A_0 A_1 \left[S_{+f_0}(f) S_{+f_1}(f) + S_{-f_0}(f) S_{-f_1}(f)\right]$	Moderate	$\lvert f_0 - f_1 \rvert = f_D$
$2A_0 A_2 \left[S_{+f_0}(f) S_{+f_2}(f) + S_{-f_0}(f) S_{-f_2}(f)\right]$	Weak	$\lvert f_0 - f_2 \rvert = 2f_D$
$2A_1 A_2 \left[S_{+f_1}(f) S_{+f_2}(f) + S_{-f_1}(f) S_{-f_2}(f)\right]$	Moderate	$\lvert f_1 - f_2 \rvert = f_D$
$2A_0 A_1 \left[S_{+f_0}(f) S_{-f_1}(f) + S_{-f_0}(f) S_{+f_1}(f)\right]$	Moderate	$f_0 + f_1 = 2f_C + f_D$
$2A_0 A_2 \left[S_{+f_0}(f) S_{-f_2}(f) + S_{-f_0}(f) S_{+f_2}(f)\right]$	Weak	$f_0 + f_2 = 2f_C + 2f_D$
$2A_1 A_2 \left[S_{+f_1}(f) S_{-f_2}(f) + S_{-f_1}(f) S_{+f_2}(f)\right]$	Moderate	$f_1 + f_2 = 2f_C + 3f_D$

Downloaded 30 Mar 2011 to 198.102.153.2. Redistribution subject to AIP license or copyright; see http://rsi.aip.org/about/rights_and_permissions

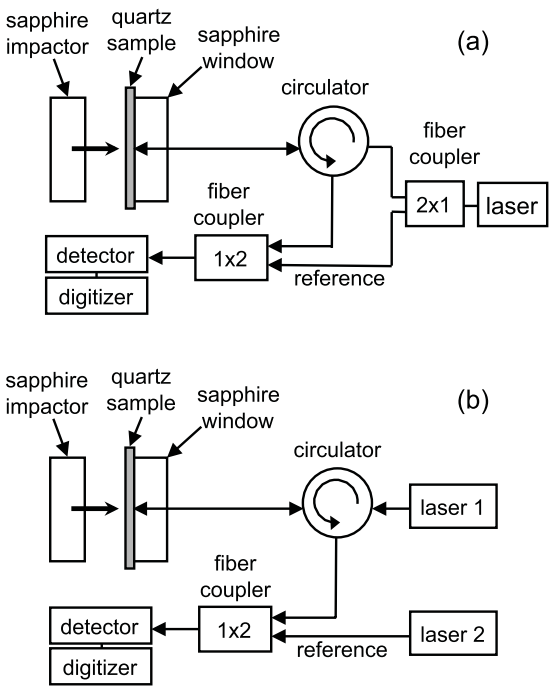

FIG. 3. Experimental layouts of (a) conventional PDV configuration and (b) frequency-conversion PDV configuration.

exterior side was either left bare, coated with antireflective film (< 0.05% at 1550 nm), or wedge-cut at 8°. Two PDV configurations were used to track reflector velocity. In both configurations, a NP Photonics "Rock" laser operating near 1550.000 nm illuminated the target. This laser also served as the reference in conventional PDV measurements, while a second "Rock" laser (tuned to a slightly longer wavelength) was used as a reference in frequency-conversion PDV measurements. Light was coupled to the target with a OZ optics focusing probe (12 mm working distance) and measured with a 12.5 GHz bandwidth receiver (sampled at 50 Gsamples/s). Signal frequency increased as the reflector moved toward the probe in both configurations, but the frequency-conversion PDV started at ∼4 GHz while the conventional PDV started at zero frequency.

IV. RESULTS AND ANALYSIS

Table II summarizes five shock experiments performed in this study. The experiments differed mainly in preparation of the free surface of the sapphire window: bare, antireflective coated, or 8° wedge. Conventional PDV was used in two experiments (Shots No. 146 and 148) while frequency-conversion PDV was used in three experiments (Shots No. 152, 155, and 170). The average impact velocity of the experiments was 207 ± 3 m/s, corresponding to a completely elastic compression (4.6 GPa) of the quartz and sapphire pieces.

The apparent initial velocities listed in Table II correspond to the mean value of the first velocity step. All of these velocity values were obtained using a Hamming window function, a time duration of 5 ns, and 1024 frequency points in the STFT analysis. The velocity variations within the initial velocity step are measured in two ways: (1) total velocity range (difference between velocity minimum and maximum) and (2) 1σ standard deviation (percentage).

A. Conventional PDV measurements

Figure 4(a) shows the STFT power spectrum of a conventional PDV measurement through a bare sapphire window (Shot No. 146) and Fig. 4(b) shows the extracted velocity using three STFT analysis time durations ($\tau = 5$, 10, and 15 ns). The velocity ringing is most severe when the smallest time duration is used. Increasing the time duration reduces the velocity ringing by narrowing the spectral functions [see Fig. 2(c)], but inherently degrades the time resolution of the measurement. Velocity ringing is essentially suppressed with the largest time duration, at a cost of a factor of 3 loss in time resolution (compared to smallest time duration). The main ringing frequency is $2f_D$ (0.384 GHz), as shown in Fig. 4(c), though ringing at f_D (0.192 GHz) is also present. Since ringing frequency is proportional to apparent velocity ($f_D = 2v^*/\lambda_0$), the extracted velocity rings faster at subsequent velocity steps.

TABLE II. Comparison of extracted velocity histories for bare, AR coated, and wedged sapphire windows in nominally similar impact experiments (≈200 m/s impact velocity). The initial velocity was determined with a Hamming window function, $\tau = 5$ ns, and 1024 frequency points. The total velocity range (minimum to maximum) and standard deviation (relative to the mean) of the extracted velocity are given as measures of ringing magnitude.

Shot No.	PDV configuration	Window back-reflection (%)	Impact velocity (m/s)	Apparent initial velocity (m/s)	Velocity range (m/s)	Standard deviation (%)
146	Conventional	7	212.4 ± 0.9	152.9	72	10.1
148	Conventional	<0.05[a]	203.4 ± 1.7	150.9	55	12.7
152	Frequency-conversion	<0.05[a]	206.8 ± 0.5	144.6	7	1.5
155	Frequency-conversion	7	207.0 ± 1.0	145.4	43	10.0
170	Frequency-conversion	<0.0001[b]	207.6 ± 1.2	146.2	5	1.2

[a]AR coated window.
[b]8° wedge window.

Downloaded 30 Mar 2011 to 198.102.153.2. Redistribution subject to AIP license or copyright; see http://rsi.aip.org/about/rights_and_permissions

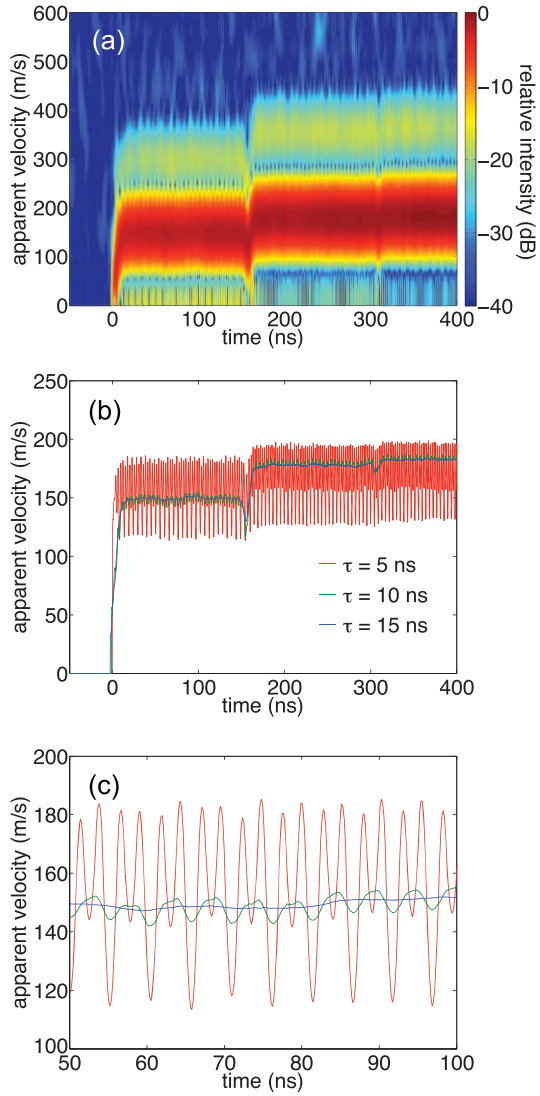

FIG. 4. (Color) Conventional PDV measurement through a bare sapphire window (Shot No. 146). (a) STFT power spectrum, (b) full velocity history, and (c) magnified velocity history.

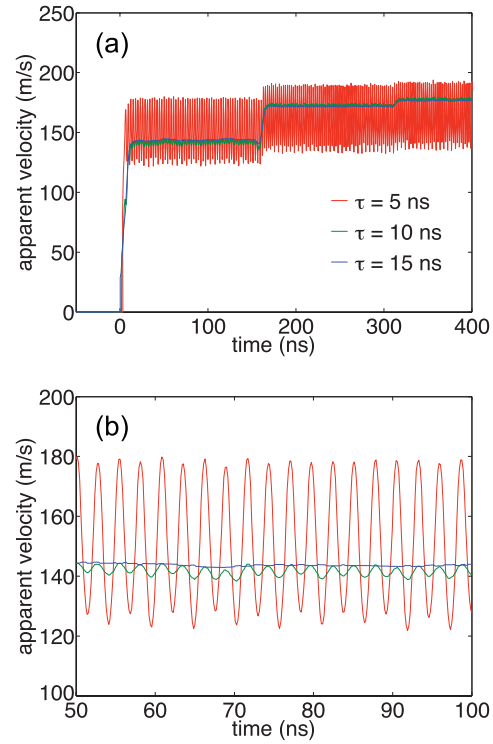

FIG. 5. (Color) Conventional PDV measurement through an antireflective coated <0.05% at 1550 nm sapphire window (Shot No. 148): (a) full velocity history and (b) magnified velocity history.

Figure 5 shows the extracted velocity of a conventional PDV measurement through an antireflective (AR) coated sapphire window (Shot No. 148) using three STFT analysis time durations ($\tau = 5$, 10, and 15 ns). Since zeroth and secondary reflections are suppressed by the AR coating, only the ringing frequency $2f_D$ due to $2A_1^2 S_{+f_1}(f) S_{-f_1}(f)$ remains. In addition to velocity ringing caused by time-dependent spectral contributions, static spectral contributions affect the accuracy of the velocity history. For example, when a small time duration is applied to Shot No. 148, its mean initial apparent velocity of 150.9 m/s (see Table II) is noticeably higher than the mean initial apparent velocities obtained with larger time durations [see Fig. 5(b)]. Referring to Fig. 2(a), a small time duration has broad spectral functions, thus the strong negative frequency contribution $A_1^2 S_{-f_1}^2(f)$ interferes with the main positive frequency spectral function and shifts the extracted velocity. Conversely, larger time durations have narrower spectral functions, so interaction with the negative frequency contribution is suppressed and the extracted velocity is more accurate.

For a time duration of 5 ns, the bare sapphire PDV measurement (Shot No. 146) has a slightly smaller standard deviation than the AR coated sapphire PDV measurement (Shot No. 148). However, the AR coated sapphire has a distinctly smaller total velocity range than the bare sapphire. Since the bare sapphire's velocity ringing is asymmetric about its mean velocity, as shown in Fig. 4(b), its standard deviation is reduced in comparison to a symmetric ringing [see Fig. 5(b)]. However, increasing the time duration to 10 ns removes the bare sapphire's ringing asymmetry, and as expected the total velocity range and standard deviation of the AR coated sapphire are better than the bare sapphire's results.

B. Frequency-conversion measurements

Figure 6 shows the extracted velocity history through a bare sapphire window with frequency-conversion PDV (Shot No. 155) using three STFT analysis time durations ($\tau = 5$, 10, and 15 ns). The frequency-conversion PDV bare sapphire velocity history's ringing [see Fig. 6(b)] is noticeably less severe than the conventional PDV result [see Fig. 4(b)], in terms of having a smaller amplitude and lower ringing frequency. With frequency-conversion PDV, negative frequency spectral functions [see Fig. 2(b)] are shifted away from the positive frequency spectral functions, thus static contributions are reduced and the accuracy of the PDV measurement

Downloaded 30 Mar 2011 to 198.102.153.2. Redistribution subject to AIP license or copyright; see http://rsi.aip.org/about/rights_and_permissions

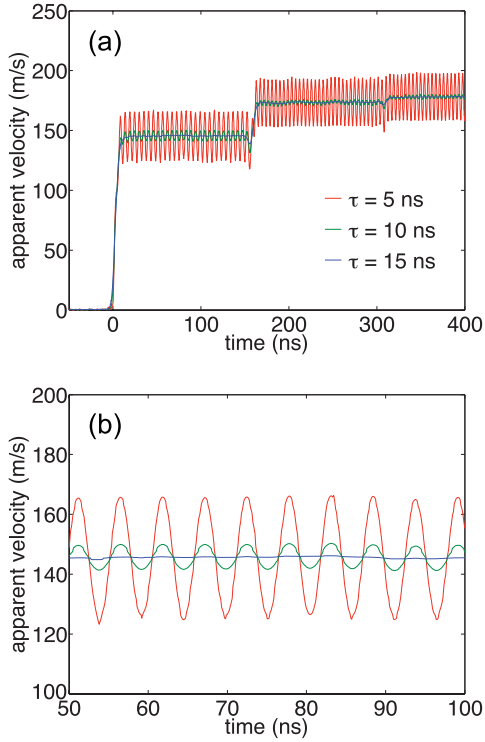

FIG. 6. (Color) Frequency-conversion PDV measurement through a bare sapphire window (Shot No. 155): (a) full velocity history and (b) magnified velocity history.

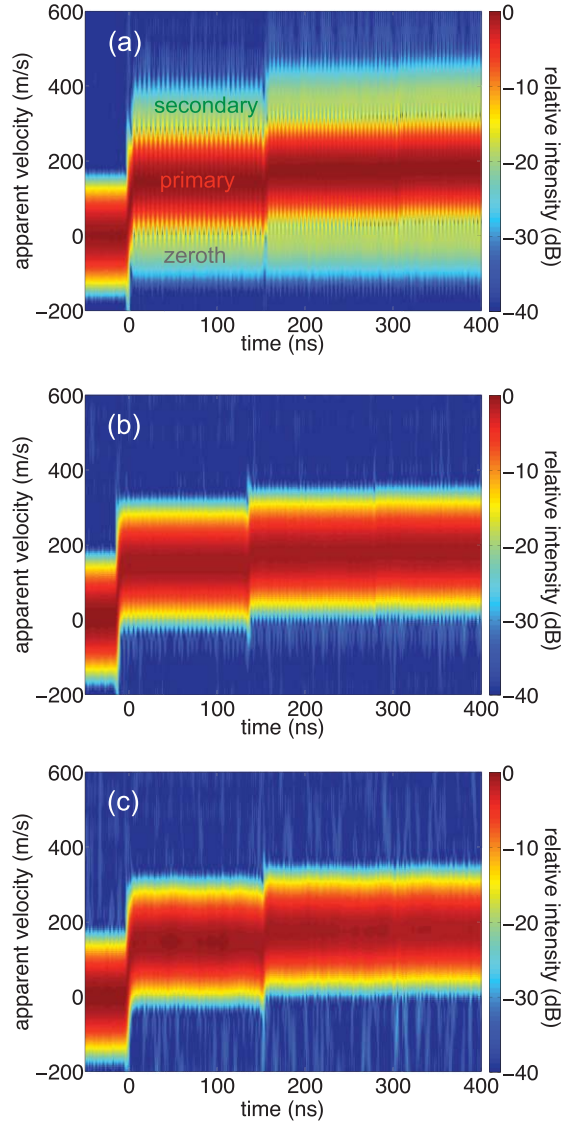

FIG. 7. (Color) STFT power spectra of frequency-conversion PDV measurements ($\tau = 5$ ns) through (a) a bare sapphire window (Shot No. 155), (b) an antireflective coated <0.05% at 1550 nm sapphire window (Shot No. 152), and (c) an 8° wedge sapphire window (Shot No. 170).

is improved. Since a conversion frequency of $f_C \approx 4$ GHz was used in these experiments, the spectral functions of the opposite-sign mixing are substantially separated from each other so their ringing contributions are reduced considerably. However, the interaction from same-sign mixing between separate reflections remains, and occurs at the Doppler shift frequency $f_D = |f_0 - f_1| = |f_1 - f_2|$.

The STFT power spectrum [see Fig. 7(a)] of the PDV signal for a bare sapphire window provides a better view of the window reflection interactions. In addition to the spectral profile of the primary reflection, other spectral profiles due to multiple Fresnel window reflections (see Fig. 1) are clearly observed. Direct removal of the additional reflections using either AR coated sapphire windows or wedge sapphire windows have been experimentally examined. Antireflective coatings of <0.5% are generally adequate for VISAR windows, but the requirements are more stringent for PDV because signals scale with field amplitude rather than intensity. For this work, a sapphire window with an AR coating of < 0.05% at 1550 nm significantly suppressed the zeroth and secondary spectral features, as shown in Fig. 7(b). Alternatively, by wedging the free surface of the window any Fresnel window reflections are deflected away from the PDV probe. For this work, an 8° wedge sapphire window was quite effective in removing the zeroth and secondary spectral features, as shown in Fig. 7(c). A drawback about the wedge window was the added complexity of alignment of the PDV probe to the angled surface.

Velocity ringing in AR coated and wedge windows was dramatically suppressed compared to the bare sapphire window results (Fig. 8). The AR coated window produced a modest level of periodic ringing (total range of 7 m/s, standard deviation of 1.5%) for 5 ns analysis duration, while the wedged window had slightly smaller variations (5 m/s velocity range, 1.2% standard deviation). The latter result is surprising because the geometry of the wedge window measurement keeps back-reflections below 0.0001%, yet the results are quite similar to the AR coated measurement. Since PDV signal magnitudes scale with electric field [Eq. (6)], velocity ringing should scale with the square root of window back-reflection; the ratio of velocity ringing magnitude to the square root of window reflectivity should be roughly constant. Based on the results in Table II, this ratio for coated sapphire is within a factor of 2 from uncoated sapphire, in qualitative agreement with how window reflections contribute to the PDV signal. However, the ratio for wedge sapphire is >30 times larger than uncoated sapphire, indicating that this ringing cannot be attributed to residual window reflections.

Downloaded 30 Mar 2011 to 198.102.153.2. Redistribution subject to AIP license or copyright; see http://rsi.aip.org/about/rights_and_permissions

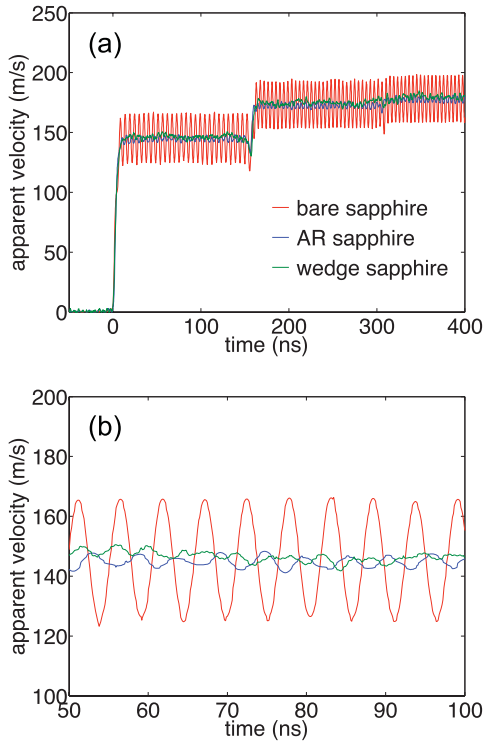

FIG. 8. (Color) Frequency-conversion PDV measurements ($\tau = 5$ ns) through a bare sapphire window (Shot No. 155), an antireflective (AR) coated <0.05% at 1550 nm sapphire window (Shot No. 152), and an 8° wedge sapphire window (Shot No. 170): (a) full velocity histories and (b) magnified velocity history.

The time-averaged power spectra in the peak state (Fig. 9) reveals a qualitative difference between the AR coated and wedge window measurements. Both measurements contain a strong central peak (the primary reflection) and a weaker peak (the zeroth reflection) at lower frequency. However, the secondary reflection peak (right of the primary peak) is present in the AR coated window measurement but absent from the wedge window measurement. This difference suggests the existence of an internal path within the PDV that allows some target light to mix with the reference laser without Doppler shifting. This can happen with imperfect fiber connections (insufficient polish angle or quality) or circulator bleed through, which directs light toward the PDV detector without reflecting from the target. The latter effect is suspected in this work because the specifications for PDV bleed through vary widely: many circulators have −30 to −40 dB bleed through, which is comparable to a 0.1% to 0.01% window reflection.

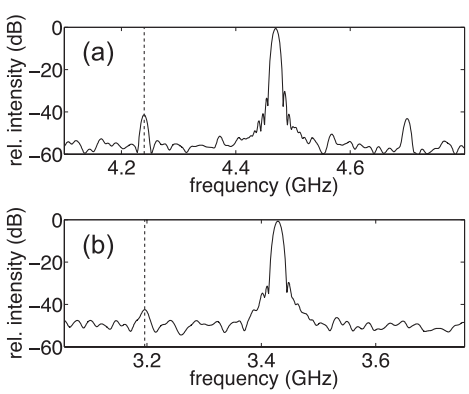

FIG. 9. Time-averaged power spectra of frequency-conversion PDV measurements through (a) an AR coated <0.05% at 1550 nm sapphire window (Shot No. 152) and (b) an 8° wedge sapphire window (Shot No. 170). Each spectrum is calculated from an ≈500 ns region after the peak velocity was reached ($t > 300$ ns in Fig. 7). The dotted line indicates the location of the zeroth reflection peak, which occurs at the frequency corresponding to zero velocity.

V. DISCUSSION

By mitigating window reflections with AR coatings and/or surface wedge, PDV resolution at $\tau = 5$ ns through a sapphire window is about 2.2 m/s (1.5%) for 145 m/s of motion. The limiting resolution[23] of PDV at this time scale (with 50 Gsamples/s and 10% signal noise) is about 0.8 m/s, so ringing is the dominant uncertainty. Ringing effects will decrease with measured velocity as adjacent optical reflections become better separated. Window correction uncertainty [0.2% at 1550 nm (Ref. 21)] is negligible in the present velocity regime, but ultimately limits resolution at high velocities.

Common rise times must be used to compare the performance of PDV and VISAR. The 10–90% rise time of a 5 ns Hamming window in PDV analysis has a rise time of 1.85 ns.[23] A VISAR with a similar rise time would have an interferometer delay of 2.31 ns, which corresponds to a limiting velocity resolution of 2.3 m/s (2% of a fringe constant). Thus, although VISAR measurements through a window may not ring as badly as PDV measurements, they are not necessarily more reliable. Furthermore, VISAR measurements require multiple detectors and a fixed time scale (the interferometer delay), while PDV requires only a single detector and the analysis time scale can be arbitrarily adjusted as desired (as in Figs. 4–6). If care is taken to minimize optical window reflections, PDV measurements are competitive with VISAR diagnostics.

VI. SUMMARY

PDV measurements through an optical window are noticeably affected by Fresnel reflections. Unless care is taken to reduce/eliminate these reflections, the extracted velocity profile rings due to interactions between multiple frequency components in the power spectrum. Frequency-conversion PDV is advantageous over conventional PDV because it spreads apart negative and positive spectral functions so they do not interfere with one another. Remaining interactions due to optical reflections require PDV windows to either be wedged or have sufficient antireflective coating. With these precautions, PDV measurements achieve time and velocity resolutions comparable to that of VISAR.

ACKNOWLEDGMENTS

The authors would like to thank the following people: Aaron Bowers and Andy Shay for building the targets, Randy Hickman and Jesse Lynch for operating the gas gun, and

Downloaded 30 Mar 2011 to 198.102.153.2. Redistribution subject to AIP license or copyright; see http://rsi.aip.org/about/rights_and_permissions

Sheri Payne for fielding the PDV diagnostic. Sandia National Laboratories is a multiprogram laboratory operated by Sandia Corporation, a wholly owned subsidiary of Lockheed Martin Corporation, for the United States Department of Energy's (DOE) National Nuclear Security Administration under Contract No. DE-AC04-94AL85000.

[1]G. R. Fowles, J. Appl. Phys. **32**, 1475 (1961).
[2]R. G. McQueen, S. P. Marsh, J. W. Taylor, J. N. Fritz, and W. J. Carter, in *High-Velocity Impact Phenomena*, edited by R. Kinslow (Academic, New York, 1970), pp. 249–417.
[3]G. Duvall and R. Graham, Rev. Mod. Phys. **49**, 523 (1977).
[4]L. M. Barker, in *Shock Waves in Condensed Matter-1983*, edited by J. R. Asay, R. A. Graham, and G. K. Straub (Elsevier, New York, 1984), pp. 217–224.
[5]J. Asay, AIP Conf. Proc. **505**, 261 (2000).
[6]J. R. Asay, T. Ao, J.-P. Davis, C. Hall, T. J. Vogler, and G. T. Gray III, J. Appl. Phys. **103**, 083514 (2008).
[7]O. T. Strand, L. V. Berzins, D. R. Goosman, W. W. Kuhlow, R. D. Sargis, and T. L. Whitworth, Proc. SPIE **5580**, 593 (2005).
[8]O. T. Strand, D. R. Goosman, C. Martinez, and T. L. Whitworth, Rev. Sci. Instrum. **77**, 083108 (2006).
[9]L. M. Barker and R. E. Hollenbach, J. Appl. Phys. **43**, 4669 (1972).
[10]W. F. Hemsing, Rev. Sci. Instrum. **50**, 73 (1979).
[11]C. F. McMillan, D. R. Goosman, N. L. Parker, L. L. Steinmetz, H. H. Chau, T. Huen, R. K. Whipkey, and S. J. Perry, Rev. Sci. Instrum. **59**, 1 (1988).
[12]D. R. Goosman, J. Appl. Phys. **46**, 3516 (1975).
[13]A. V. Oppenheim and R. W. Schafer, *Discrete-time Signal Processing* (Prentice Hall, Englewood Cliffs, NJ, 1989).
[14]D. Gabor, J. Inst. Electr. Eng. **93**, 429 (1946).
[15]F. Harris, Proc. IEEE **66**, 51 (1978).
[16]A. R. Valenzuela, G. Rodriguez, S. A. Clarke, and K. A. Thomas, Rev. Sci. Instrum. **78**, 013101 (2007).
[17]M. B. Zellner, M. Grover, J. E. Hammerberg, R. S. Hixson, A. J. Iverson, G. S. Macrum, K. B. Morley, A. W. Obst, R. T. Olson, J. R. Payton, P. A. Rigg, N. Routley, G. D. Stevens, W. D. Turley, L. Veeser, and W. T. Buttler, J. Appl. Phys. **102**, 013522 (2007).
[18]N. R. Routley, E. Price, P. T. Keightley, J. C. F. Millett, N. K. Bourne, E. N. Brown, and G. T. Gray III, AIP Conf. Proc. **955**, 1131 (2007).
[19]P. Mercier, J. Bénier, P. A. Frugier, A. Sollier, M. R. L. Gloahec, E. Lescoute, J. P. Cuq-Lelandais, M. Boustie, T. de Rességuier, A. Claverie, E. Gay, L. Berthe, and M. Nivardc, AIP Conf. Proc. **1195**, 581 (2009).
[20]P. A. Frugier, P. Mercier, J. Bénier, J. Veaux, M. Debruyne, C. Rion, and E. Dubreuil, Proc. SPIE **7429**, 742913 (2009).
[21]B. J. Jensen, D. B. Holtkamp, P. A. Rigg, and D. H. Dolan, J. Appl. Phys. **101**, 013523 (2007).
[22]The continuous Fourier transform is presented here for conceptual clarity, though in practice a discrete analysis (e.g., the fast Fourier transform) is used.
[23]D. H. Dolan, Rev. Sci. Instrum. **81**, 53905 (2010).
[24]D. H. Dolan, Sandia Report SAND2008-3871 (Sandia National Laboratories), 2008.

Downloaded 30 Mar 2011 to 198.102.153.2. Redistribution subject to AIP license or copyright; see http://rsi.aip.org/about/rights_and_permissions